Non-rigid Registration with Reliable Distance Field for Dynamic Shape Completion

Kent Fujiwara[1], Hiroshi Kawasaki[2], Ryusuke Sagawa[3], Koichi Ogawara[4] and Katsushi Ikeuchi[1]
[1]The University of Tokyo, Japan [2]Kagoshima University, Japan
[3]National Institute of Advanced Industrial Science and Technology, Japan
[4]Wakayama University, Japan
kfuji,ki@cvl.iis.u-tokyo.ac.jp, kawasaki@ibe.kagoshima-u.ac.jp
ryusuke.sagawa@aist.go.jp, ogawara@sys.wakayama-u.ac.jp

Abstract

We propose a non-rigid registration method for completion of dynamic shapes with occlusion. Our method is based on the idea that an occluded region in a certain frame should be visible in another frame and that local regions should be moving rigidly when the motion is small. We achieve this with a novel reliable distance field (DF) for non-rigid registration with missing regions. We first fit a pseudo-surface onto the input shape using a surface reconstruction method. We then calculate the difference between the DF of the input shape and the pseudo-surface. We define the areas with large difference as unreliable, as these areas indicate that the original shape cannot be found nearby. We then conduct non-rigid registration using local rigid transformations to match the source and target data at visible regions and maintain the original shape as much as possible in occluded regions. The experimental results demonstrate that our method is capable of accurately filling in the missing regions using the shape information from prior or posterior frames. By sequentially processing the data, our method is also capable of completing an entire sequence with missing regions.

1. Introduction

Acquisition of 3D information is becoming a common practice in various fields, from projects with cultural background [14, 18] that try to capture sites, to applications in robotics [6, 4] that require 3D information to locate where robots or vehicles are. Conventional research mainly focused on acquisition of static scenes. However, with the advent of compact and affordable sensors, capturing dynamic scenes and objects is on the rise [22, 9, 12]. Acquisition of dynamic 3D data is significant in situations where marker-based motion capture systems cannot be used.

Figure 1: Shape completion using our method. The source shape on the left is transformed to the target shape at the center using reliable distance field information.

There are various methods that attempt to acquire the entire shape of dynamic objects [9]. This is usually conducted by placing multiple sensors or cameras to fully capture the target shape from all angles. However, when shapes are undergoing deformation, occlusion is inevitable and even multiple sensors may not be able to capture regions that are occluded. There are hole-filling methods that attempt to solve this problem by inserting points or surface patches. These methods are proposed for static single frame range data and do not utilize information from the entire sequence.

We claim that a dynamic shape should be completed using the information available from neighboring frames in the sequence as much as possible. We base this idea on an assumption that an occluded region in a frame should be visible in another. Prior work has mainly tackled the problem by fitting a template to fill the occluded regions [2] or by gradually merging similar frames to establish a template, then transforming the template to each frame [23].

We approach the problem of shape completion through non-rigid registration. We claim that the pairwise corre-

spondence between neighbouring frames provides significant information regarding how the shape is moving and where points on the surface will go. We assume that transformations of small local regions on the dynamic shape, visible or not, can be approximated by rigid transformation. We take advantage of these characteristics to complete missing regions on dynamic shapes.

We achieve this by representing shapes with a novel distance field (DF). We determine unreliable regions in the DF disrupted by occlusions on the original data. We fit a pseudo-surface onto the original data, and compute the DFs of the original data as well as the pseudo-surface. We compare the two DFs and identify regions with significant difference. We then discard them to create a reliable DF for surface with occlusion. We emphasize that the pseudo-surface is only used to calculate the new DF, and is not at all used to fill holes, as it cannot fully capture details.

In order to robustly conduct registration between frames while maintaining the original shape as much as possible, we adopt a locally-rigid globally non-rigid registration method [8]. The method considers a shape as a group of local structures that move rigidly to find the best matching location on the surface. The overall deformation is determined by the final location of the free form deformation (FFD) [21] control points, each of which is embedded at the center of each local structure. The newly proposed DF allows the registration method to match shapes with occlusions without distorting the original data.

In order to conduct shape completion, we sequentially select a frame and its subsequent frame, and apply the non-rigid registration method with the reliable DF representation. We merge the two frames and use the result as the source shape for the following frame. We repeat the process until the end of the sequence to produce a complete model. We then propagate the final result to prior frames to obtain a complete shape for each frame in the sequence. This can be done by directly applying the proposed non-rigid registration method. Here, we use the complete shape as the source and partial data at each frame as the target shape.

We demonstrate the effectiveness of the method using the models from Gall *et al*. [9]. We remove some parts from a pair of frames and apply our method to observe whether the registration results are accurate. We also test the method on multiple frames to demonstrate that our method is capable of completing a sequence of moving shape.

2. Related Work

There are various methods for filling in occluded regions on a static 3D shape taken from various perspectives [11]. Some directly work to edit polygon information [17], while others use a volumetric approach to fill the surface [20].

There are also many attempts to reconstruct complete dynamic shapes. One main type of hole-filling methods for dynamic data is based on templates. Carranza *et al*. [2] use a human model to estimate the human pose from silhouettes from multiple cameras. Anguelov *et al*. [1] use human models with different pose and body characteristics to learn the deformation for each triangle patch. The method then estimates the optimal model that best fits the input point set. This model has been used in other methods to reconstruct human bodies from partial data [24]. Li *et al*. [15] deform a template to input meshes, and then integrate the details on the original input meshes to the transformed template to recover the details. Recently, more case-specific methods have been proposed [5] to handle various garments and body shapes and provide results with higher quality than fitting a general model. However, these templates are usually unavailable when considering general shapes in motion.

Methods without templates have recently been proposed to handle dynamic shapes with occlusion. Method for articulated shapes have been proposed by Pekelny and Gotsman [19]. This method, however, requires rough manual segmentation of the data. Chang and Zwicker [3] propose a method that simultaneously solves for the alignment of shapes and the segmentation of rigid parts. Zeng *et al*. [25] introduce a deformation graph to complete articulated shape models. The method deforms a deformation graph to range data taken at different times and gradually integrates the resulting graphs. These methods are designed for articulated objects, and cannot be directly applied to general shapes undergoing non-rigid transformation.

Hole filling methods for non-rigid shapes have also been proposed. Wand *et al*. [23] attempt to form a hierarchy of frame pairs and merge the pairs of shapes. This process is repeated until one final shape is obtained, which is then transformed to each shape in the sequence. Instead of creating hierarchy of frames, our method attempts to handle frames sequentially. By assuming that the shapes are locally rigid in between frames, our method processes the data from the beginning to the end of the sequence to robustly reconstruct dynamic shapes.

Another method by Li *et al*. [16] attempts to overcome this issue by first constructing a hole-filled model for each frame. The complete mesh from one mesh is transformed to neighboring frames and are combined using Poisson surface reconstruction. The details are synthesized using normal maps. Our method avoids filling in holes at each frame, as reconstructed surface may greatly vary depending on the size of the holes. We achieve this by propagating the visible shape in one frame to other frames within the sequence while maintaining their shape as much as possible.

3. Non-rigid Registration with Local Transformations

Starting at the beginning of the sequence, we deform each frame to the subsequent frame by non-rigid registra-

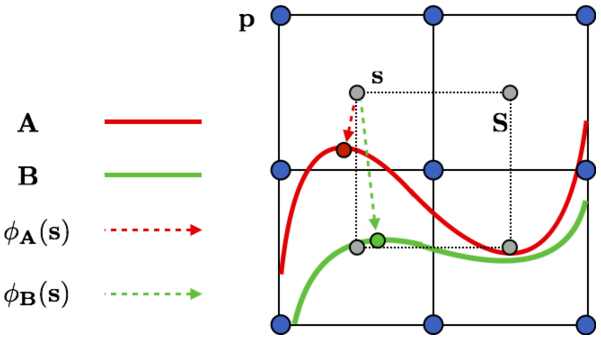

Figure 2: Configuration of the registration method. The source and target shapes $\mathbf{A}$ and $\mathbf{B}$ are enclosed in a grid consisting of FFD control points $\mathbf{p} \in \mathbf{P}$. Each control point is embedded in a sampling region $\mathbf{S}$, which determines the local rigid transformation. The transformation is obtained by minimizing the difference between distance values $\phi_{\mathbf{A}}(\mathbf{s})$ and $\phi_{\mathbf{B}}(\mathbf{s})$, measured at sampling points $\mathbf{s}$.

tion. We base our method on the locally rigid globally non-rigid registration method [8, 7], which is intended to be used for data without occlusion. For simplicity, we explain the method in 2D, but the method can easily be extended to 3D data by adding another dimension.

We consider the problem of deforming a source shape $\mathbf{A}$ to a target shape $\mathbf{B}$. The method first sets up a grid over $\mathbf{A}$ consisting of FFD control points $\mathbf{p} \in \mathbf{P}$ and a sampling grid. Each sampling region $\mathbf{S}$ in the sampling grid contains partial DF information of shape $\mathbf{A}$ and a control point at the center. Similar to the template matching method in image registration, these sampling regions act as templates which transform to the most similar location on the target. Fig. 2 shows the configuration of the registration method.

The error function can be defined as:

$$E = \int\int \alpha(\mathbf{p})\Big(\phi_{\mathbf{B}}\big(\mathbf{p}+\mathbf{t}(\mathbf{p})\big) - \phi_{\mathbf{A}}(\mathbf{p})\Big)^2 + \lambda\Big(1-\alpha(\mathbf{p})\Big)\Big(\mathbf{t}_x(\mathbf{p})^2 + \mathbf{t}_y(\mathbf{p})^2\Big)d\mathbf{x}\,, \quad (1)$$

where $\phi(\mathbf{x})$ indicates the distance field value at a point $\mathbf{x}$ and λ is the weight balancing the error term and the smoothness term. The weight $\alpha(\mathbf{x}) = \frac{1}{1+e^{n(l-k)}}$ is a sigmoid function that determines the importance of point $\mathbf{p}$ in space, defined relative to the distance to the surface, k is the midpoint of the sigmoid determined by the gap between control points, and $l = \frac{1}{2}(\phi_{\mathbf{A}}(\mathbf{x}) + \phi_{\mathbf{B}}(\mathbf{x}))$ is the average of the source and the target DF at point $\mathbf{x}$. The size of the FFD grid and the parameters for the sigmoid function are automatically determined by the size of the input shape.

To solve for the transformations $\mathbf{t}$, the error function above is firstly discretized and points $\mathbf{s}$ are introduced to each sampling region to obtain the distance values in each region. Then, the Euler-Lagrange equation is derived for each control point from Eq. (1). This is expressed as

$$\alpha(\mathbf{p})\frac{1}{n}\sum_{i}^{n}\Big(\phi_{\mathbf{B}}\big(\mathbf{p}+\mathbf{s}_i+\mathbf{t}(\mathbf{p})\big) - \phi_{\mathbf{A}}(\mathbf{p})\Big) \cdot \frac{\partial}{\partial \mathbf{t}}\phi_{\mathbf{B}}\big(\mathbf{p}+\mathbf{s}_i+\mathbf{t}(\mathbf{p})\big) + \lambda\Big(\alpha_x(\mathbf{p})\mathbf{t}_x(\mathbf{p}) + \alpha_y(\mathbf{p})\mathbf{t}_y(\mathbf{p})\Big) - \lambda\Big(\big(1-\alpha(\mathbf{p})\big)\Delta\mathbf{t}(\mathbf{p})\Big) = 0\,, \quad (2)$$

where $\mathbf{t} = (u, v)$ is the translation of a point $\mathbf{x}$, $\mathbf{t}_x(\mathbf{x}) = \frac{\partial}{\partial x}\mathbf{t}(\mathbf{x})$, and $\mathbf{t}_y(\mathbf{x}) = \frac{\partial}{\partial y}\mathbf{t}(\mathbf{x})$. $\mathbf{p} = (x, y)$ is the FFD control point and $\mathbf{s}_i = (s_i^x, s_i^y)$ is the sampling point in the sampling region surrounding each control point.

Finally, a point $\mathbf{a} = (a_x, a_y)$ on surface $\mathbf{A}$ is deformed by cubic B-spline FFD. The deformation is computed by adding transformation from each sampling region $\mathbf{t}_{pq} = (u_{pq}, v_{pq})$ to the corresponding control point:

$$\mathbf{T}(a_x, a_y) = \sum_p \sum_q B_p(s)B_q(t)\Big(\mathbf{p}_{pq} + \mathbf{t}_{pq}\Big)\,. \quad (3)$$

This method is effective for registration of shapes with similar structures in the vicinity of each other. However, it cannot handle situations where there are missing features or occlusions in the data, as the distance field is calculated without considering where the occlusion is. This forces the method to deform excessively in order to minimize the difference between distance fields of the source and target shapes, as demonstrated in Fig. 3. Therefore, the method cannot be applied to dynamic shapes with occlusion.

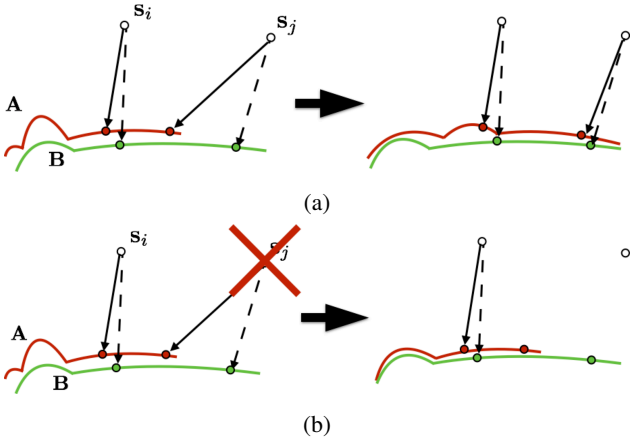

Figure 3: Registration strategy of source shape $\mathbf{A}$ and target $\mathbf{B}$. The previous method (a) attempts to pull the shape to close a hole as the difference between distance values at region around $\mathbf{s}_j$ is large. Our method (b) defines unreliable regions and avoids using distance values near holes.

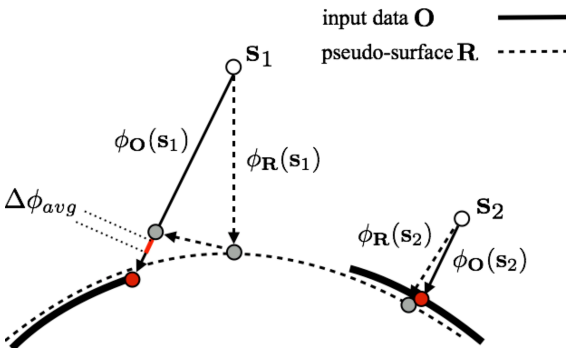

Figure 4: Calculation of reliable region in the distance field. From sampling points $\mathbf{s}$ in space, the distance to the nearest point in each data is calculated. If the difference between the distance values from input data and the pseudo-surface is above $\Delta\phi_{avg}$, the region will be removed from the registration process. In this case, data from $\mathbf{s}_1$ will be removed.

4. Proposed Method

We propose a non-rigid registration method for dynamic shapes with occlusion. In order to handle missing data, we first propose a reliable distance field for shape preserving non-rigid registration method. Then, we propose a shape completion process for handling partial dynamic shapes.

4.1. Non-rigid Registration with Reliable Distance Field

We propose a method to determine the reliable regions in the DF. Fig. 3 shows an example comparing the previous and the proposed method using reliable distance fields. In the previous method, distance field is calculated without the knowledge of holes. The method tries to minimize the difference between the two DFs. However, in regions around point $\mathbf{s}_j$, the discrepancy between the two distance values is large, as there is a hole in the surface on top, indicated by the red curve. As a result, the surface is pulled to the right, in an attempt to minimize the difference at every sampling point. Our method identifies such region where accurate distance field cannot be calculated due to occlusion.

We achieve this by comparing the original data with a pseudo-surface constructed using the points from the original data. Fig. 4 shows our strategy for determining reliable regions. For each frame in the sequence, we first fit a pseudo-surface $\mathbf{R}$ onto each input shape $\mathbf{O}$ using the poisson surface reconstruction method [13]. We transfer the geometry of the input to the pseudo-surface as much as possible during this process. We then calculate the DF for both the input data shape and the pseudo-surface, denoted as $\phi_{\mathbf{O}}$ and $\phi_{\mathbf{R}}$ respectively. Finally, we obtain the average of differences between two DFs at each sampling point defined in the registration method, which we call $\Delta\phi_{avg}$.

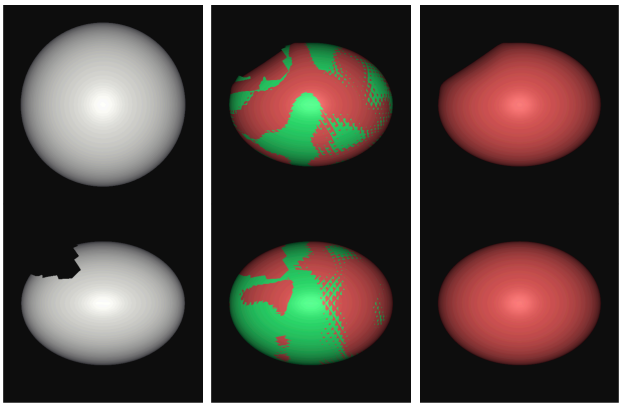

(a) (b) (c)

Figure 5: Comparison of registration results. (a): Source (top) and target (bottom) shapes. (b): Registration results. Source: red, target: green. (c): Source shape after deformation. Top: previous method, bottom: proposed method. The proposed method maintains the character of the source shape as much as possible while matching existing parts.

Using this average of differences, we construct our newly proposed reliable distance field for registration. For each sampling point in the sampling regions, we calculate the absolute difference between the distance from the sampling point to the original data, and the distance from the sampling point to the pseudo-surface. If this absolute difference is larger than the average difference, we discard the distance information. In other words, the reliable distance at sampling point $\mathbf{s}_i$ is defined as:

$$\phi'(\mathbf{s}_i) = \begin{cases} \phi_{\mathbf{O}}(\mathbf{s}_i) & |\phi_{\mathbf{O}}(\mathbf{s}_i) - \phi_{\mathbf{R}}(\mathbf{s}_i)| < \Delta\phi_{avg} \\ 0 & otherwise \end{cases} \tag{4}$$

We calculate this distance for each sampling point, and denote the final updated field as ϕ'.

Using the reliable distance field, we modify the non-rigid registration in the previous section and apply it to partial shapes. We replace the original DF in Eq.(1) with the newly updated distance field.

We modify the Euler-Lagrange equation to

$$\begin{aligned} \alpha(\mathbf{p})\frac{1}{m}\sum_{i}^{m}\Big(\phi'_{\mathbf{B}}(\mathbf{p}+\mathbf{s}_i+\mathbf{t}(\mathbf{p})) - \phi'_{\mathbf{A}}(\mathbf{p})\Big) \\ \cdot \frac{\partial}{\partial \mathbf{t}}\phi'_{\mathbf{B}}(\mathbf{p}+\mathbf{s}_i+\mathbf{t}(\mathbf{p})) \\ + \lambda\Big(\alpha_x(\mathbf{p})\mathbf{t}_x(\mathbf{p}) + \alpha_y(\mathbf{p})\mathbf{t}_y(\mathbf{p})\Big) \\ - \lambda\Big((1-\alpha(\mathbf{p}))\Delta\mathbf{t}(\mathbf{p})\Big) = 0\,, \end{aligned} \tag{5}$$

where m is the number of sampling points at which distance values to both the source and target shapes were reli-

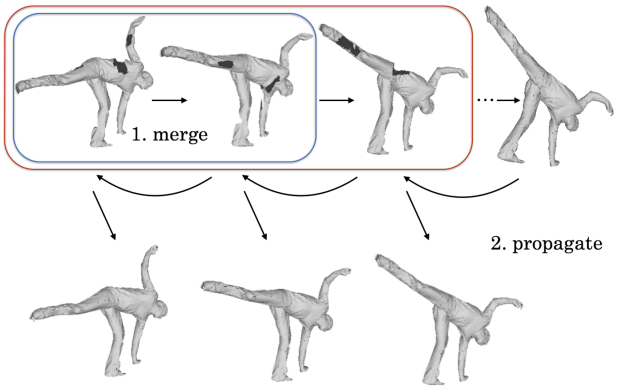

Figure 6: Shape completion procedure. First, the partial shapes from two consecutive frames are aligned and merged using the proposed method. This is repeated until the end of the sequence. Then, the final complete shape at the end is propagated back to the previous frames. This is conducted by sequentially registering the complete shape to previous partial data.

able. In other words, we exclude the sampling points with unreliable information from calculation of transformations to only consider the information from existing shapes. Note that both the DFs of the source and target shapes are replaced with the reliable ones. We then apply the transformations to the FFD control points as in Eq. 3. Fig. 5 shows an example of the effects from the proposed method.

4.2. Shape Completion

Once the registration between the first two frames is complete, we merge the two data. When merging overlapping regions, we prioritize the information from the latter frame, as it should be more accurate compared to the transformed shape from the prior frame. We can achieve this by transferring geometric data from the prior frame to the latter, or by methods such as algebraic point set surfaces [10]. The merged result would then be used as the source shape and is aligned and merged to the the third frame. This process is repeated until the end of the sequence to obtain a complete shape. This is shown as the merging process in Fig. 6. When some regions are unobservable throughout the sequence, we apply Poisson surface reconstruction [13] to the final result to obtain the shape with no missing region.

We then sequentially transform the final shape to the preceding frames to obtain the complete shape in each frame. This can be achieved by using the proposed non-rigid registration method. Here, we set the source shape as the complete shape in frame n and the target as the partial shape in frame $n-1$. Then, the transformed result will be reused as a source shape to be matched to the partial shape in frame $n-2$. This is repeated frame by frame to avoid drastic deformation as the sequence may involve large motion. As a result, we can obtain a complete shape for each of the frames. This corresponds to the propagation process in Fig. 6.

5. Experiments

5.1. Registration Accuracy

To evaluate the validity of our method, we first applied our method to the dataset provided by Gall *et al*. [9]. We selected nearby frames from sequences in the dataset and compared the registration accuracy between the previous method by Fujiwara *et al*. [8, 7] and the proposed method.

We selected frames 186 and 191 from "dance", 65 and 70 from "handstand", and 55 and 60 from "skirt" data. These frames contain large changes in the shapes. We then randomly removed approximately 10% of points from each shape so that when registered and merged, they should produce a complete shape. We compared the average distance between points from the registration results and their closest points on the ground truth from the dataset. For the sake of comparison, we also registered the original complete surfaces using the method by Fujiwara *et al*.

The results are shown in Fig. 7. The shape in column (a) is transformed to the shape in (b) using the registration methods, and they are then merged together. The shapes in (c) are the final results using the registration method proposed by Fujiwara *et al*., the shapes in (d) are the final results from the proposed method. Finally, column (e) shows the original target shapes without missing data. The average distance between points on the merged results and the closest points on the original shape is shown in Table 1.

The images in the first row are from the "dance" dataset. The merged result from the method by Fujiwara *et al*. contains some residual error at both sides of the person, where the source and target shapes do not exist. Our method was able to bring the source shape and the target shape together by maintaining the source shape as much as possible and fill the gap. The second row shows the results from the "handstand" dataset. The missing area on the target shape caused the result from the previous method to cave in. Our method was able to remove this unreliable region from registration and bring the shapes together. The same effect can be observed in the case of "skirt" dataset shown in the bottom row, where we aggressively removed half of the structure from the abdomen of the dancer. This can also be seen from the comparison of residual error in Table 1.

The results demonstrate that our method is capable of bringing dynamic shapes into alignment even when there are large holes in the data. The examples show that the overall shape can be accurately completed when the holes on two shapes are mutually exclusive.

(a) Source (b) Target (c) Fujiwara *et al*. [7] (d) Proposed (e) Original Data

Figure 7: Registration results. (a) Source shape, (b) target shape, (c) merged results from Fujiwara *et al*., (d) merged results from proposed method, (e) original target data.

5.2. Shape Completion Using Range Data Sequence

In order to demonstrate the effectiveness of the proposed method for completion of sequential data, we conducted another experiment using the "dance" sequence from the same dataset. From frames 90 to 110, we extracted every 5 frames for the experiment. We manually removed points randomly from each data, as shown in the top row of Fig. 8.

The bottom row of Fig. 8 shows the results from shape completion process. First, the frames were sequentially registered and merged, resulting in a complete shape at frame 110. Then, we sequentially transformed the complete shape at frame 110 ((e) bottom) to the shapes at preceding frames and merged the data. The results show that our registration strategy is able to gather information from multiple frames and complete the shapes accurately.

5.3. Limitations

Although in most cases, missing data can successfully be merged with our method, our method fails when knowl-

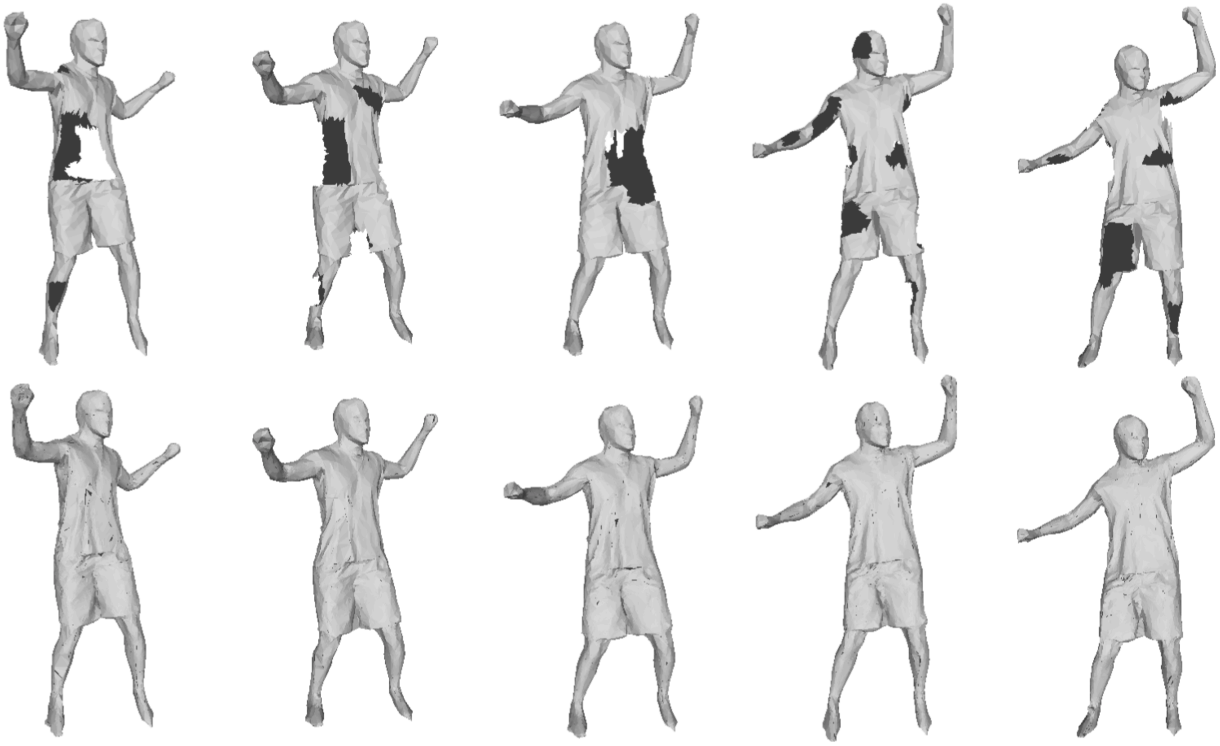

(a) Frame 90 (b) Frame 95 (c) Frame 100 (d) Frame 105 (e) Frame 110

Figure 8: Result from shape completion. The frames are sequentially aligned from first to last, leading to a complete shape in frame 110 ((e),bottom row). The complete shape is then deformed back sequentially to each of the incomplete shapes to fill in the holes, resulting in shapes at the bottom row of (a) - (d).

data	Method		
	[7]	Proposed	Complete
Dance	7.053111	5.981080	4.653706
Skirt	6.390158	3.767186	3.488573
Handstand	4.694146	4.187120	3.787354

Table 1: Average distance between points on the final shapes and the closest points on the original shapes.

edge regarding the target shape is required. An example is shown in Fig. 9. In this case, taken from frames 177 and 182 in the "skirt" sequence, the skirt is removed from the target shape. The proposed method tried to complete the shape by maintaining the source shape as much as possible, leading to a reasonable merged result. However, the dancer is taking a step forward during these frames, causing the skirt to flare. As this is highly unpredictable from just two frames, the result from our method could not completely match the original data in this region.

Similarly, our method cannot accurately match shapes when the majority or an entire segment of some part is missing. This is due to the fact that we do not predict the movement of the parts from the sequence. These errors can be reduced by estimating motion from multiple frames, which we would like to address in future work.

6. Conclusion

We proposed a non-rigid registration method using reliable distance fields to mitigate the effect of holes on dynamic shapes. We considered the local motions during a short interval of time to be rigid transformations, which was effective in completing missing regions using information from neighboring frames.

Future work will be on analyzing the sequence of dynamic data to determine the quality of shapes. A human body would deform differently from clothes, and the results should improve if such information were available. Another direction would be to consider more than two frames for estimation of global movement. This should be useful for completion of parts that are totally obscure in some frames.

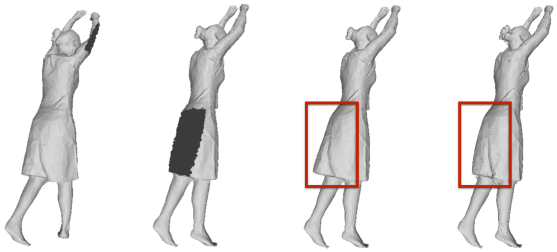

(a) source (b) target (c) Original (d) Proposed

Figure 9: Limitation of the proposed method. The rear part of the skirt was completely removed from the target shape in (b). Our method tried to maintain the structure of (a) as much as possible, leading to a flatter result, as shown in (d), compared to the original data in (c).

References

[1] D. Anguelov, P. Srinivasan, D. Koller, S. Thrun, J. Rodgers, and J. Davis. Scape: Shape completion and animation of people. *ACM Trans. Graph.*, 24(3):408–416, 2005.

[2] J. Carranza, C. Theobalt, M. A. Magnor, and H.-P. Seidel. Free-viewpoint video of human actors. In *In Proceedings of SIGGRAPH*, pages 569–577, 2003.

[3] W. Chang and M. Zwicker. Global registration of dynamic range scans for articulated model reconstruction. *ACM Trans. Graph.*, 30(3):26:1–26:15, 2011.

[4] A. Davison, I. Reid, N. Molton, and O. Stasse. MonoSLAM: Real-time single camera SLAM. *Pattern Analysis and Machine Intelligence, IEEE Transactions on*, 29(6):1052–1067, 2007.

[5] E. de Aguiar, C. Stoll, C. Theobalt, N. Ahmed, H.-P. Seidel, and S. Thrun. Performance capture from sparse multi-view video. *ACM Trans. Graph.*, 27(3):98:1–98:10, 2008.

[6] M. Dissanayake, P. Newman, S. Clark, H. Durrant-Whyte, and M. Csorba. A solution to the simultaneous localization and map building (SLAM) problem. *IEEE Transactions on Robotics and Automation*, 17(3):229–241, 2001.

[7] K. Fujiwara, K. Nishino, J. Takamatsu, and K. Ikeuchi. Non-rigid registration using local rigid transformations. In *The University of Tokyo CVL Technical Report*, number 1, 2013.

[8] K. Fujiwara, K. Nishino, J. Takamatsu, B. Zheng, and K. Ikeuchi. Locally rigid globally non-rigid surface registration. In *Proceedings of IEEE International Conference on Computer Vision*, pages 1527–1534, 2011.

[9] J. Gall, C. Stoll, E. de Aguiar, C. Theobalt, B. Rosenhahn, and H.-P. Seidel. Motion capture using joint skeleton tracking and surface estimation. In *Proceedings of IEEE Conference on Computer Vision and Pattern Recognition*, pages 1746–1753, 2009.

[10] G. Guennebaud and M. Gross. Algebraic point set surfaces. *ACM Trans. Graph.*, 26(3), 2007.

[11] T. Ju. Fixing geometric errors on polygonal models: A survey. *Journal of Computer Science and Technology*, 24(1):19–29, 2009.

[12] N. Kasuya, R. Sagawa, R. Furukawa, and H. Kawasaki. One-shot entire shape scanning by utilizing multiple projector-camera constraints of grid patterns. In *The IEEE International Conference on Computer Vision (ICCV) Workshops*, 2013.

[13] M. Kazhdan, M. Bolitho, and H. Hoppe. Poisson surface reconstruction. In *Proceedings of the Fourth Eurographics Symposium on Geometry Processing*, pages 61–70, 2006.

[14] M. Levoy, K. Pulli, B. Curless, S. Rusinkiewicz, D. Koller, L. Pereira, M. Ginzton, S. Anderson, J. Davis, J. Ginsberg, J. Shade, and D. Fulk. The digital Michelangelo project: 3D scanning of large statues. In *Proceedings of SIGGRAPH*, pages 131–144, 2000.

[15] H. Li, B. Adams, L. J. Guibas, and M. Pauly. Robust single-view geometry and motion reconstruction. *ACM Trans. Graph.*, 28(5):175:1–175:10, 2009.

[16] H. Li, L. Luo, D. Vlasic, P. Peers, J. Popović, M. Pauly, and S. Rusinkiewicz. Temporally coherent completion of dynamic shapes. *ACM Trans. Graph.*, 31(1):2:1–2:11, 2012.

[17] P. Liepa. Filling holes in meshes. In *Proceedings of the 2003 Eurographics/ACM SIGGRAPH Symposium on Geometry Processing*, pages 200–205, 2003.

[18] D. Miyazaki, T. Oishi, T. Nishikawa, R. Sagawa, K. Nishino, T. Tomomatsu, Y. Takase, and K. Ikeuchi. The great Buddha project: Modeling cultural heritage through observation. In *Modeling from Reality*, volume 640, pages 181–193. 2001.

[19] Y. Pekelny and C. Gotsman. Articulated object reconstruction and markerless motion capture from depth video. *Computer Graphics Forum*, 27(2):399–408, 2008.

[20] R. Sagawa and K. Ikeuchi. Hole filling of a 3D model by flipping signs of a signed distance field in adaptive resolution. *IEEE Transactions on Pattern Analysis and Machine Intelligence*, 30(4):686–699, 2008.

[21] T. Sederberg and S. Parry. Free-form deformation of solid geometric models. In *Proceedings of the 13th annual conference on Computer graphics and interactive techniques*, SIGGRAPH '86, pages 151–160, 1986.

[22] X. Su and Q. Zhang. Dynamic 3-D shape measurement method: A review. *Optics and Lasers in Engineering*, 48(2):191 – 204, 2010.

[23] M. Wand, B. Adams, M. Ovsjanikov, A. Berner, M. Bokeloh, P. Jenke, L. Guibas, H.-P. Seidel, and A. Schilling. Efficient reconstruction of nonrigid shape and motion from real-time 3D scanner data. *ACM Trans. Graph.*, 28(2):15:1–15:15, 2009.

[24] A. Weiss, D. Hirshberg, and M. Black. Home 3D body scans from noisy image and range data. In *Proceedings of IEEE International Conference on Computer Vision*, pages 1951–1958, 2011.

[25] M. Zeng, J. Zheng, X. Cheng, and X. Liu. Templateless quasi-rigid shape modeling with implicit loop-closure. In *IEEE Conference on Computer Vision and Pattern Recognition*, pages 145–152, 2013.